JOURNAL OF GEOPHYSICAL RESEARCH, VOL. 95, NO. B5, PAGES 6629–6645, MAY 10, 1990

Behavior of the Southernmost San Andreas Fault During the Past 300 Years

KERRY E. SIEH AND PATRICK L. WILLIAMS[1]

Division of Geological and Planetary Sciences, California Institute of Technology, Pasadena

Surficial creep occurs at low rates along the Coachella Valley segment of the San Andreas fault, which has not produced a large earthquake during the period of historical record. Geodetic data indicate, however, that the crust adjacent to this segment of the San Andreas fault is accumulating strain at a high rate. Furthermore, neotectonic and paleoseismic data indicate that the fault does produce very large earthquakes every two to three centuries. In view of its long-term behavior, the occurrence of creep along the surficial trace of the fault in the Coachella Valley is of particular interest. Along two short reaches of the San Andreas fault in the Coachella Valley, measurements of offset geological deposits and man-made structures and from alignment arrays and creep meters show that slip rates of 2–4 mm/yr near Indio and near the Salton Sea have persisted for the past three centuries. This slow aseismic surficial creep is not a transient precursor to seismic failure of this segment of the fault. We suggest that the Coachella Valley segment of the San Andreas fault creeps in its upper few kilometers. This behavior may be due to tectonically induced high pore pressures in the coarse sediments that abut the fault.

INTRODUCTION

The San Andreas fault is divisible into four segments, based on its historical behavior (inset to Figure 1). The 200-km-long dormant, southern segment is distinct from the other three in that it has generated neither a great earthquake nor high rates of creep during the period of historical record.

The implications of the historical dormancy of this segment for its future behavior have been unclear. Twenty years ago, *Allen* [1968] proposed that even though it was active, the southern segment might release strain by creep and moderate earthquakes rather than by sudden slippage in large or great earthquakes. Others have argued that this segment is currently locked and slips primarily during great earthquakes [*Raleigh et al.*, 1982; *Lindh*, 1983; *Sykes and Nishenko*, 1984].

Geologic and geodetic measurements made over the past 20 years provide evidence that the latter opinion is correct. Geological slip rates of about 25 mm/yr determined near Indio and near Cajon Pass leave little doubt about the segment's high rate of slip during the past several thousand years [*Keller et al.*, 1982; *Weldon and Sieh*, 1985; *Sieh*, 1986]. Furthermore, wide-aperture geodetic measurements of the past two decades indicate high rates of strain in the crustal blocks adjacent to the southern San Andreas fault that are consistent with the millennial rate [*Savage et al.*, 1981, 1986; *Prescott et al.*, 1987]. Measurements that Allen started two decades ago show that aseismic fault creep occurs at rates that are an order of magnitude lower than the average millennial rate [*Keller et al.*, 1978; *Louie et al.*, 1985]. Furthermore, evidence of past seismogenic fault ruptures with at least 2 m of dextral slip [*Sieh*, 1986; *Williams*, 1989] indicate that this fault segment does generate earthquakes of very large magnitude. This, plus information in this paper about interseismic fault slippage, suggests that as a first-order approximation, this segment is locked and will generate large earthquakes.

These data suggest that the southern segment of the San Andreas fault behaves like the segments that produced the great 1906 and 1857 earthquakes. If the rate of strain accumulation along this segment has been steady during the past three centuries, an average of 6–8 m of surficial fault slip could be expected during a future large earthquake.

We sought to determine whether low-level creep is a transient or a long-term property of the southern segment. If low-level creep has been occurring only during the past few decades, it might well represent incipient failure precursory to a great earthquake, as has been suggested by *Stuart* [1986]. The onset of such behavior along faults or segments elsewhere in the world might then be monitored as a vanguard of major earthquakes on those structures. If, on the other hand, low-level creep has been continuous during the entire period since the last prehistoric great earthquake, it is not a precursory signal.

The presentation and analysis of data in this paper are divided into two major sections, each with three subsections. We first discuss evidence for fault slip rates near Indio over periods of one decade to 3 centuries. Second, we discuss evidence for fault creep from sites on the eastern shore of the Salton Sea, also over periods of 10–300 years.

HISTORICAL SLIP RATE DATA FROM NEAR INDIO

Slip rate at the Dillon Road and Indio Hills alignment arrays. In 1967, C. R. Allen began to establish small arrays of markers and creep meters across several faults in southern California. These arrays and creep meters have enabled measurement of creep and coseismic fault slip. These measurements are made at seven locations that straddle strands of the San Andreas fault zone in the Coachella Valley (squares in Figure 1). Detailed discussion of data from these sites is given by *Keller et al.* [1978] and *Louie et al.* [1985]. Average rates of slip vary from 0 to 4 mm/yr between sites.

The Indio Hills and the Dillon Road arrays (northwesternmost two solid squares on Figure 1) are within a few kilometers of older, datable, geological, and man-made markers offset across the fault. Their history, therefore, is of

[1]Now at Lawrence Berkeley National Laboratory, Berkeley, California.

Paper number 89JB03523.
0148-0227/90/89JB-03523$05.00

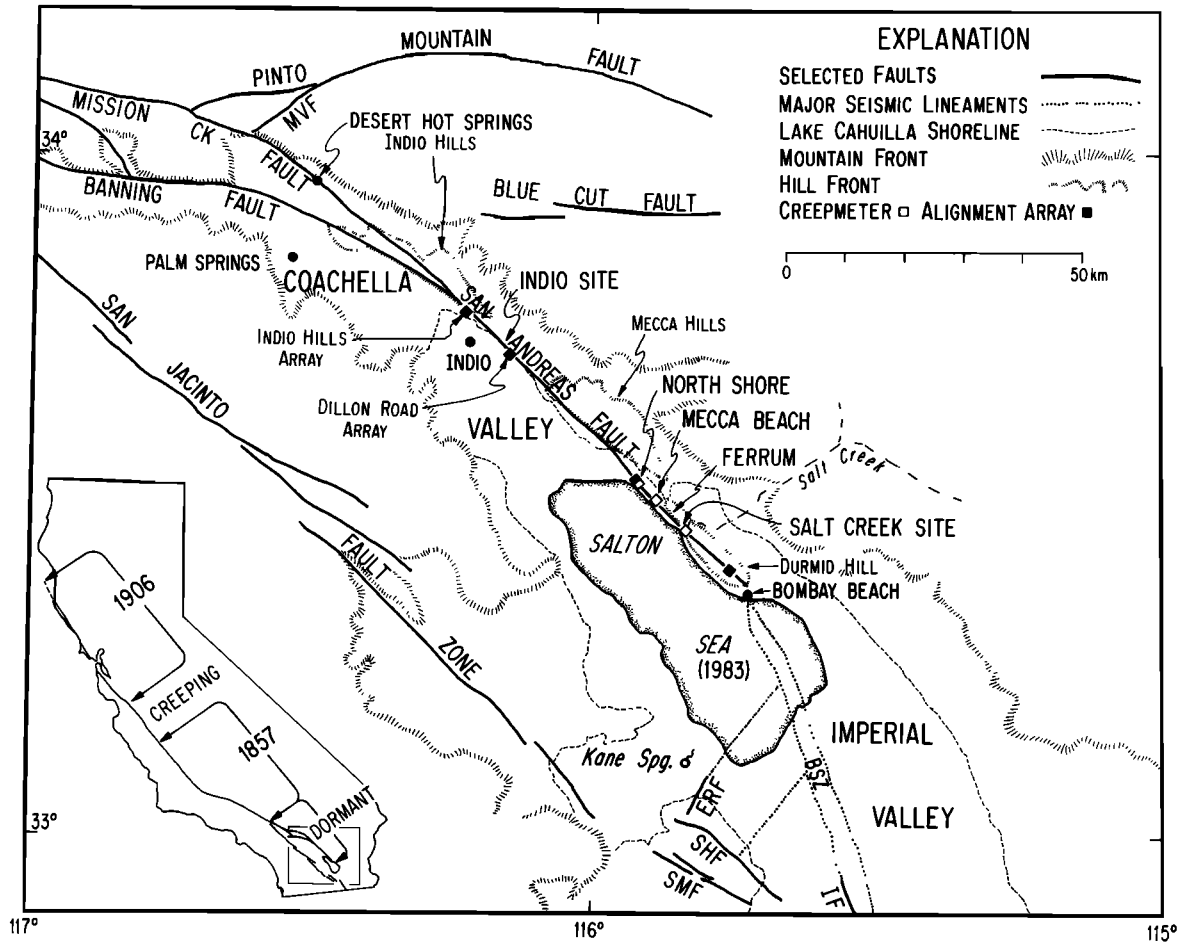

Fig. 1. Tectonic setting of the southernmost San Andreas fault and locations of places mentioned in the text. Alignment array and creep meter sites are, from north to south, Indio Hills, Dillon Road, North Shore, Mecca Beach, Salt Creek, and Bertram. Active faults in the vicinity of the southernmost San Andreas fault include the Brawley seismic zone (BSZ), Elmore Ranch fault (ERF), Imperial fault (IF), Morongo Valley fault (MVF), Superstition Hills fault (SHF), and Superstition Mountain fault (SMF). Inset shows four segments of the San Andreas fault that can be distinguished by their historical behavior. Geometry of faulting from *Clark* [1984], *Jennings* [1975], and *Williams and Magistrale* [1989].

particular interest to us. *Louie et al.* [1985] report that between June 1977 and November 1982, the Indio Hills alignment array recorded creep at an average rate of 1.8 ± 0.6 mm/yr. Between April 1970 and February 1984, the Dillon Road array recorded an average creep rate of 2 ± 1 mm/yr.

Offset of a concrete canal across the San Andreas fault near Indio. No reference lines or small-aperture arrays were constructed across the San Andreas fault in the Coachella Valley for the purpose of monitoring fault activity until 1967. For this reason, any measurement of fault slippage that occurred prior to 1967 must utilize other reference features that straddle the fault zone. One such feature is a concrete-lined channel that crosses the fault near Indio, between the Indio Hills and Dillon Road alignments arrays (Figure 1). This channel, which is called Wasteway 3, was constructed in 1948 and 1949 by the Coachella Water District, according to T. Levy of the Coachella Water District on June 10, 1985. It is almost perpendicular to the Coachella Canal and to the San Andreas fault (Figure 2). Aerial photographs taken in 1930, before construction of the wasteway and major modification of the surrounding landscape, enable location of the intersection of the wasteway and fault zone to within a few meters. The photographs show that in the vicinity of the intersection, the fault zone is quite straight and uncomplicated.

Our surveys of the top of the inside edge of both the southeastern and northwestern wall of the wasteway show that, over a zone of about 20 m, the walls are offset about 68 mm (Figure 3). This bend is visible on the southeastern wall of the wasteway, but it is obscured by vegetation on the northwestern wall. The 20-m width of the zone of deformation probably exceeds the actual width of the fault zone in the sediments because the canal liner is constructed of reinforced concrete, the strength of which must lead to a distribution of deformation. Irregularities in the wall result in a measurement uncertainty of about 10%. This is a conservative estimate of error, especially for the southeastern wall. The 68 ± 7 mm offset accumulated in the 36 years between construction in 1948/1949 and our surveys in the spring of 1985. The average rate of slip is, therefore, 1.9 ± 0.2 mm/yr.

This rate is indistinguishable from the rates of creep of 1.8 ± 0.6 and 2 ± 1 measured at the Indio Hills and the Dillon Road alignment arrays. The simplest interpretation, therefore, is that creep has been occurring along this reach of the fault at a steady rate of about 2 mm/yr for at least the past

four decades. Clearly, however, the low precision of the measurements, especially at the Dillon Road array, precludes recognition of small fluctuations in creep rate over this time period.

SLIP RATE DATA FOR THE PAST 300 YEARS NEAR INDIO

East of Indio, the San Andreas fault intersects the shorelines of several late Holocene lakes that inundated much of the Coachella and Imperial valleys. These lakes are collectively called Lake Cahuilla. Extensive excavations of lacustrine, fluvial, and aeolian sediments at this intersection have revealed an interesting history of both prehistoric fault activity and lake fillings and drainings [*Sieh*, 1986]. Pertinent to the theme of this paper is the history of faulting at this site since the latest lake began to dry up, about 300 years ago.

At the Indio site, the San Andreas fault zone is about 50 m wide and consists of several discrete faults (Figure 4). The fault zone cuts obliquely across a sand bar constructed principally of the beach deposits of the most recent eight lakes. The strand labeled 1 in Figure 4 has accommodated about 90% of the slip across the zone since about A.D. 1000 [*Sieh*, 1986, also manuscript in preparation, 1990]. Fault 2 has experienced an order of magnitude less slip in the same time period. Together, these two faults account for about 30 mm/yr of the total slip rate. Lacustrine sands cut by faults 3 and 4 were removed during construction of the Coachella Canal about 40 years ago, so their most recent slip history is indeterminate. Nevertheless, slip on these faults are probably very small, because the rate determined for faults 1 and 2, alone, is equal to or slightly greater than the rate determined elsewhere for the entire fault zone [*Weldon and Sieh*, 1985; *Keller et al.*, 1982].

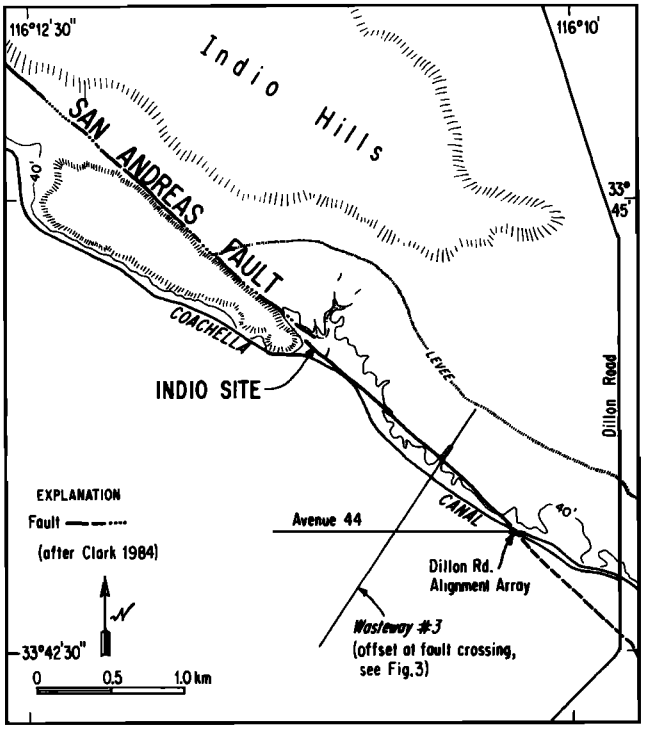

Fig. 2. Wasteway 3 crosses the San Andreas fault at a high angle, about a kilometer northwest of the Dillon Road alignment array and about a kilometer southeast of the Indio paleoseismic site. In the region of the wasteway, the fault trace is quite linear and uncomplicated. Fault trace is from *Clark* [1984].

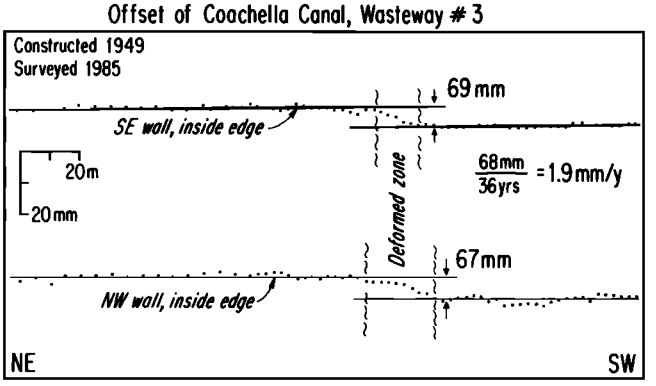

Fig. 3. Offset of Wasteway 3. Surveyed points are along the top of the inside edge of the concrete wasteway. Sold lines represent visual best fit to data points.

The most important feature of the Indio site, for the purpose of this paper, is the broad alluvial channel that bisects the bar at the fault crossing (southeastern edge of Figure 4). During the most recent highstand of the lake, the sand bar extended across the site of the channel. Mapping of numerous artificial exposures shows that the channel was cut through the bar after waters of the lake receded from the site, during the latest desiccation of the lake. The channel probably was cut soon after the level of the lake began to lower, because the bar blocked drainage of this major stream, which drains several square kilometers at the southern end of the Indio Hills.

Offset fluvial bed and channel wall. Some of the fluvial deposits within this channel are offset by faults 1 and 2. At locality A, within the channel, fault 1 offsets a tan, massive, sand bed about 1 m thick (Figure 5). On its northwestern margin, the deposit lies against a nearly vertical buttress unconformity that is cut into a slightly older channel deposit. The northwestern edge of the channel is offset about 1.2 m. The thalweg of the channel deposit is a well-defined feature that is offset about 1.1 m. The southeastern edge of the deposit is a less well defined fluvial erosional unconformity cut after deposition of the bed. It appears to be offset about 0.8 m, but because of its poor definition, we will not use it in our calculations below. Farther southeast, within younger channel deposits, the fault offsets a grain-size facies variation about 1.1 m. The average of the three well-defined offsets in Figure 5 is 1.1 ± 0.1 m. The uncertainty reflects not only the variability among the four offsets but also the spacing of the vertical exposures that were used to documents the offsets.

The northwesternmost edge of the channel in Figure 4 is offset about 950 mm by fault 1 at locality B. Figure 6 is a structure contour map that illustrates this offset. Matching of slopes across the fault zone is not straightforward, but restoration of 950 mm of offset produces the best matches of both the steepest and the flattest portions of the channel wall. The imperfect match probably reflects the fact that control for the contour map was from vertical exposures spaced about ten centimeters apart. The offset of the channel wall is more clearly depicted in Figure 7. Figure 7 shows a

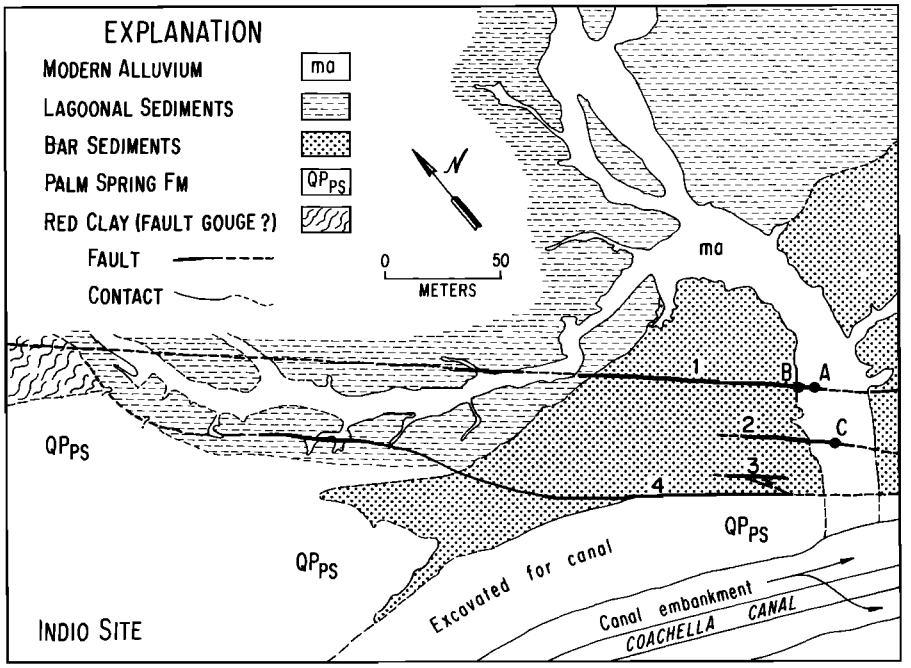

Fig. 4. Simplified Indio site map showing locations of four fault strands (1, 2, 3, and 4) and locations (A, B, C), where displacements that postdate the latest filling of Lake Cahuilla have been measured. See Figure 1 for location of the site.

pair of vertical aerial stereophotographs of a balsa-wood model of the offset, constructed from Figure 6.

Fault 2 offsets channel deposits much less than fault 1. Offsets along the portion of the fault shown in Figure 4 range between 0 and 30 mm. At locality C, fluvial deposits of the channel display a dextral offset of 30 mm (K. E. Sieh, unpublished data, 1990). Northwest of locality C, several cuts reveal no offset of channel deposits, and even the latest deposits of the latest lake, which are older than the channel deposits, are not offset. These offsets are so small that they are not significant in calculating the average slip rate below.

Age of the offset deposits and channel wall. In order to calculate a slip rate from the offsets just described, the age of the offset features must be determined. A maximum rate of deposition can be inferred from the fact that the offset bed and the channel wall postdate deposits of the latest lake. The most recent filling of Lake Cahuilla drowned vegetation growing at the Indio site that yielded a radiocarbon age on peat of 214 ± 33 years B.P. This corresponds to three calendric dates, A.D. 1641–1684, 1725–1807, and 1933–1955. (see Appendix 1). Only the oldest of these date ranges is plausible, because the younger ranges conflict with historical information. The youngest range is impossible by de Anza's observation that no lake existed at the time of his visits in 1774 and 1775 [*Bancroft*, 1884; *Bolton*, 1930]. In order for there to have been no lake at that time, lake waters must have begun to recede from the Indio site decades before 1774. Using the rate of evaporation of the Salton Sea for the period 1907–1913 (that is, 1.55 m/yr) complete evaporation of the lake from its elevation of 12 m at the Indio site to the basin floor, 85 m below sea level, would take about 63 years (see Appendix 2). Thus the lake could not have been full

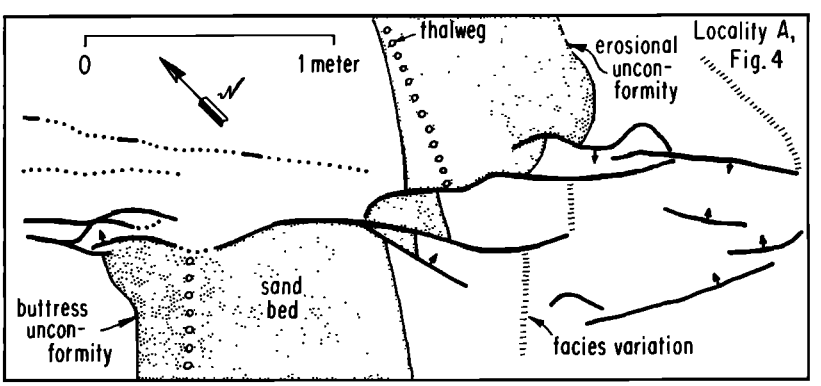

Fig. 5. Map view of locality A (see Figure 4) at the Indio site where a fluvial sand bed is offset about 1 m. Map is constructed from data gathered in vertical exposures cut perpendicular to the fault at about 10-cm intervals. This sand bed was deposited in a fluvial channel soon after the waters of the latest lake had dropped below an elevation of about 8 m above sea level.

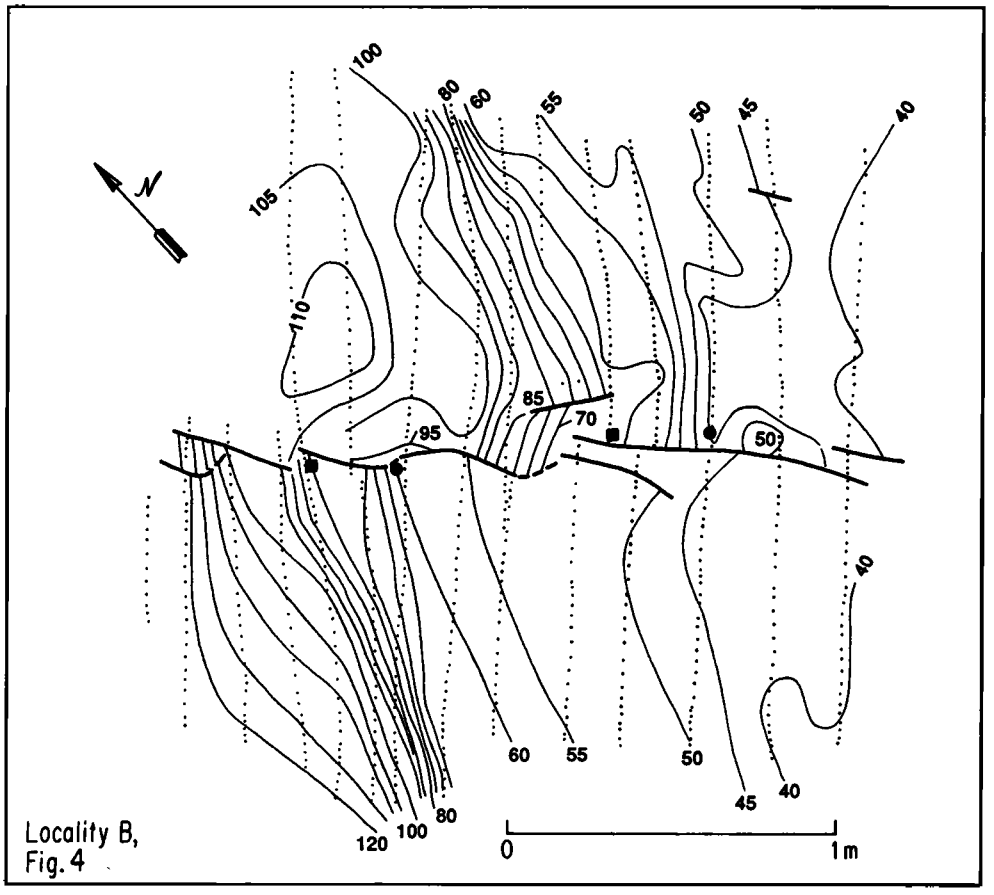

Fig. 6. Structure contour map of the channel wall at locality B, where it is offset about 95 cm. Contours are drawn in 10-cm intervals upon the base of massive, poorly sorted light gray channel sands at the top of the northwestern flank of the channel. Channel is cut into bar sands of the latest lake. Dotted lines indicate traces of mapped vertical exposures at base of channel. The best reference lines, indicated by the balls and squares, are offset about 96 and 93 cm, respectively.

during any part of the period 1725–1807 or, for that matter, any time after about 1711. This leaves 1641–1684 as the only plausible range of dates for the filling of the latest lake. The date of filling is, obviously, the oldest possible date for the inception of desiccation. Thus the inception of the desiccation of the lake is constrained by radiocarbon dates and historical observation to within the period A.D. 1641–1711, that is, A.D. 1676± 35.

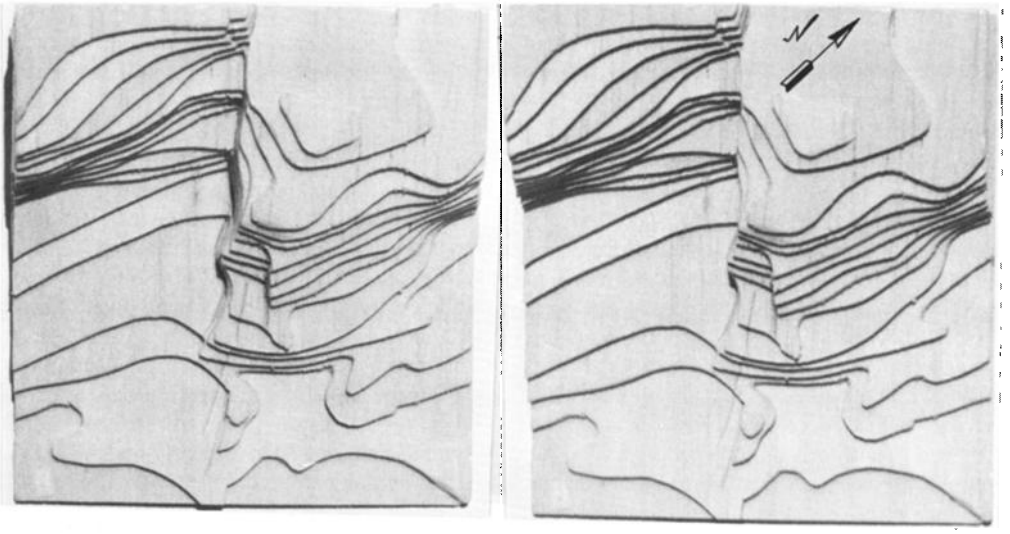

Fig. 7. Vertical aerial stereophotographs of balsa model of offset channel wall. Model was constructed from structure contours shown in Figure 6.

We believe that this date range also closely approximates the date of the channel deposits, because we surmise that the stream that cut the channel across the bar did so soon after the lake waters had receded. This is a logical deduction, given that once the site was dry, the lake bar blocked waters that the stream collected from an area of several square kilometers upstream from the lakeshore. Flash floods would likely have ponded water behind the bar soon after desiccation of the site. This would have led to sudden overtopping of the bar and rapid incision of the channel. This inference is supported by the presence of very fragile cobbles and small boulders of lacustrine and silt within the offset channel deposits. Hence we conclude that the offset channel deposits date from the latter half of the seventeenth or earliest eighteenth century.

Constraints on the slip rate at Indio. Given these constraints on the age of the offset, the average slip rate of the San Andreas fault near Indio can be calculated. The five measured offsets of 93, 96, 104, 110, and 120 cm have an average value of 1.05 ± 0.1 m. This offset accumulated in 308 ± 35 years, so the average slip rate has been 3.4 ± 0.7 mm/yr for the past three centuries [*Taylor*, 1982, p. 49]. Determination of significant contributions to slip from faults 3 and 4, destroyed by canal construction, or a younger date for the channel deposits would lead to a calculation of a higher rate. We discount the latter possibility for the reasons given above.

Historical Slip Rates From the Northeastern Flank of the Salton Sea

Modern slip rate. Determination of the average slip rate for the past three centuries has also been possible across the San Andreas fault on the northeastern flank of the Salton Sea. For this reason, we are particularly interested in the alignment array and creepmeter records along this 30-km stretch.

Two alignment arrays and three creep meters currently measure slip along this part of the fault (five squares in Figure 1). The creep meter at Salt Creek has been in operation for too short a period to determine a meaningful average rate of slip. The North Shore creep meter and alignment array have recorded no measurable slippage since their installation in 1969 and 1970 [*Louie et al.*, 1985; *S. F. McGill*, oral communication, 1988], even though slippage of about 7 mm was observed in the days following the Borrego Mountain earthquake of April 1968 [*Allen et al.*, 1972]. The Bertram alignment array, within a kilometer of the southern terminus of the San Andreas fault, has recorded a slip rate of about 1 mm/yr since its installation in 1969.

The Mecca Beach creep meter has recorded an average rate of about 4 mm/yr since its installation in 1981. Figure 8 shows that this creep has occurred principally as discrete events in 1984, 1986, and 1987. Although no data were recorded prior to the 1981 Westmorland earthquake, data collected subsequently suggest that slip occurred at Mecca Beach in association with that event. Assuming this to be the case, the average slip rate at Mecca Beach is 3.9 mm/yr.

Average rate of slip during the twentieth century. Accidental diversion of the waters of the Colorado River into the Imperial and Coachella valleys in 1905 has provided an opportunity for determination of the average rate of slip of the San Andreas fault during the past 80 years. The diversion

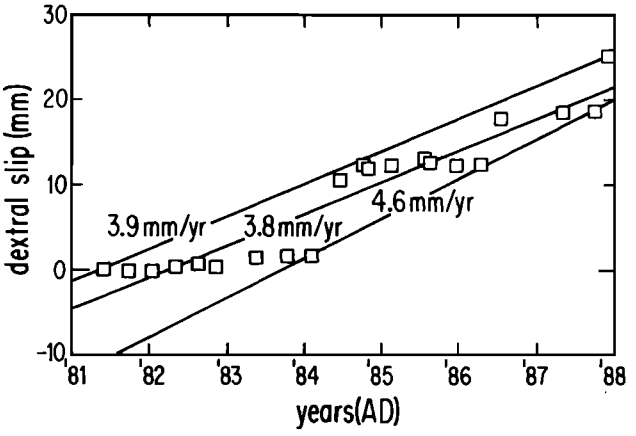

Fig. 8. Readings of the Mecca Beach creep meter indicate that creep has been occurring as discrete events and at an average rate of about 4 mm/yr since its installation in 1981.

resulted in the creation of the Salton Sea in the lowest part of the valley [*Cory*, 1913]. Before the river could be rerouted, the surface of the Salton Sea had risen to an elevation of 59.6 m below sea level. This caused the lake to flood the channel of Salt Creek (Figure 1) and deposit lacustrine sediment across the fault trace there. Offset of the lacustrine beds reveals the average slip rate of the fault during the twentieth century.

Figure 9 displays the geometry of the shoreline and fault in the Salt Creek embayment. The fault zone is well-defined as the boundary between the lacustrine Borrego and fluvial Shavers Well formations. These indurate Pleistocene and Plio-Pleistocene units commonly display folds and minor faults and steep to moderate dips. Locally overlying these rocks, within the embayment of Salt Creek, are unconsolidated fluvial, aeolian and lacustrine gravel, sand, and clay, predominantly of Holocene age. Natural and man-made exposures of these young sediments in shallow gullies revealed the left-stepping en echelon fault strands shown on Figure 9. Additionally, cairns placed in October 1979 indicate the locations of fault strands that experienced a few millimeters of dextral slip after the Imperial Valley earthquake.

At the location labeled "1907 slip site" in Figure 9, we excavated the historical shoreline deposits in order to determine the magnitude of their offset. This site is at a shallow drainage close to the 1907 highstand of the Salton Sea. Exposures of the San Andreas fault at the site and nearby indicate that slippage there is limited to a narrow zone.

Excavation of exposures at the site revealed a channel cut into a massive, poorly sorted, pebbly sand (Figure 10). The degree of sorting of the sand and its massive character indicate that it is a debris flow deposit. The channel is filled with a well-sorted, fine to medium lacustrine sand that contains prominent steeply dipping laminae. This sand appears to be have been deposited beneath the surface of the lake in a channel that was cut prior to submergence. Pieces of milled wood and other clearly historical flotsam contained within the unit prove that the unit is historical. The age of the lacustrine channel fill is very narrowly constrained. The surface of the lake stood at or above the level of the top of the deposit (−61.2 m) for only 20 months, that is, from

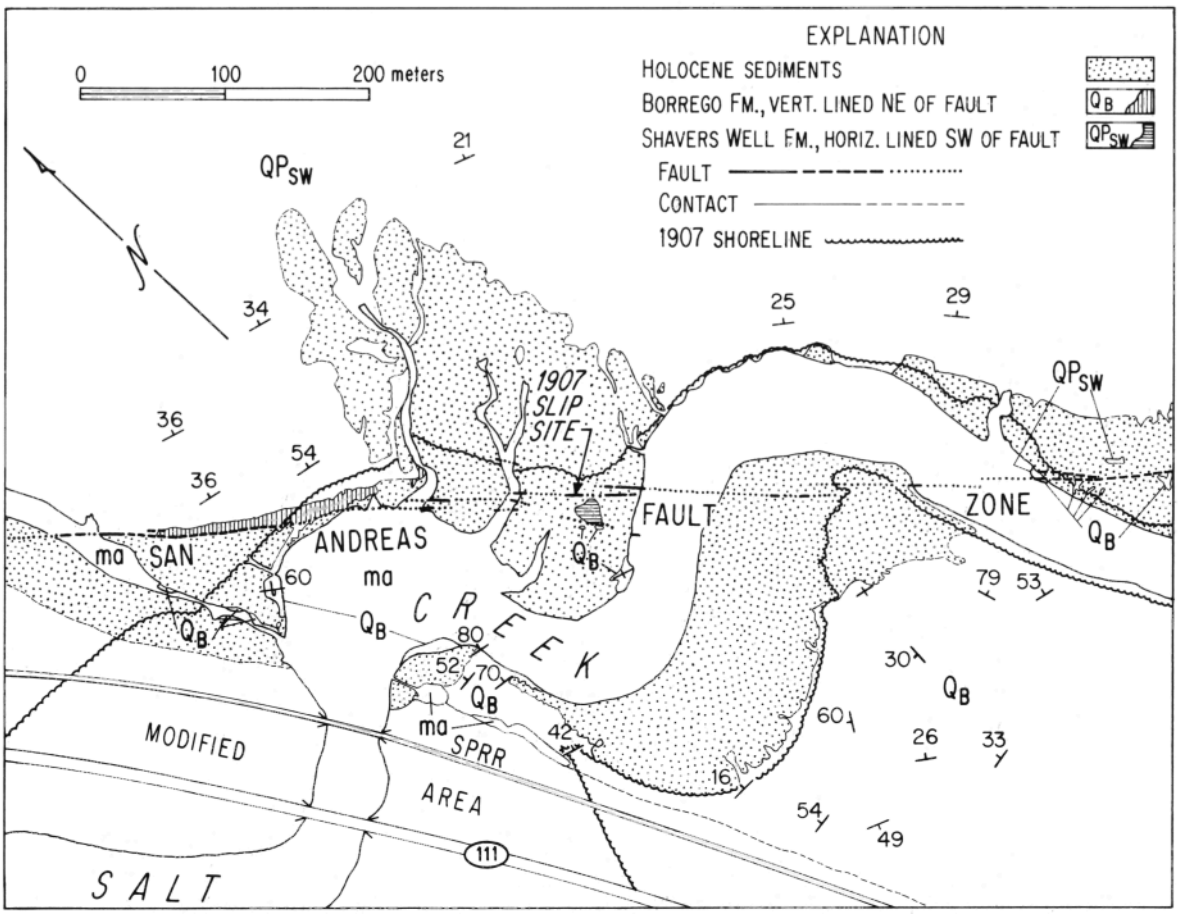

Fig. 9. Geological map of the lower reach of the Salt Creek drainage. The waters of the Salton Sea invaded the drainage in 1907 and left lacustrine sediment that has been offset subsequently by the San Andreas fault.

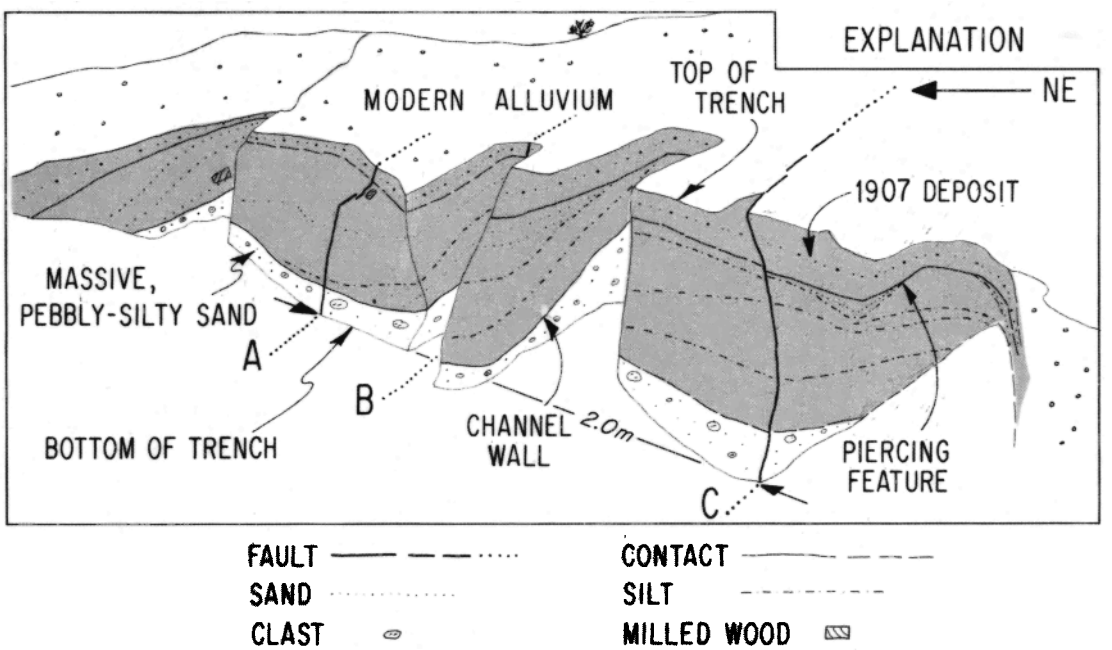

Fig. 10. Sketch (from photograph) of channel deposits excavated near the 1907-high-water level of the Salton Sea. View is to the east. The channel flowed from the upper left to the lower right. Lacustrine sand that filled the channel in 1907 was supplied primarily from the southeast.

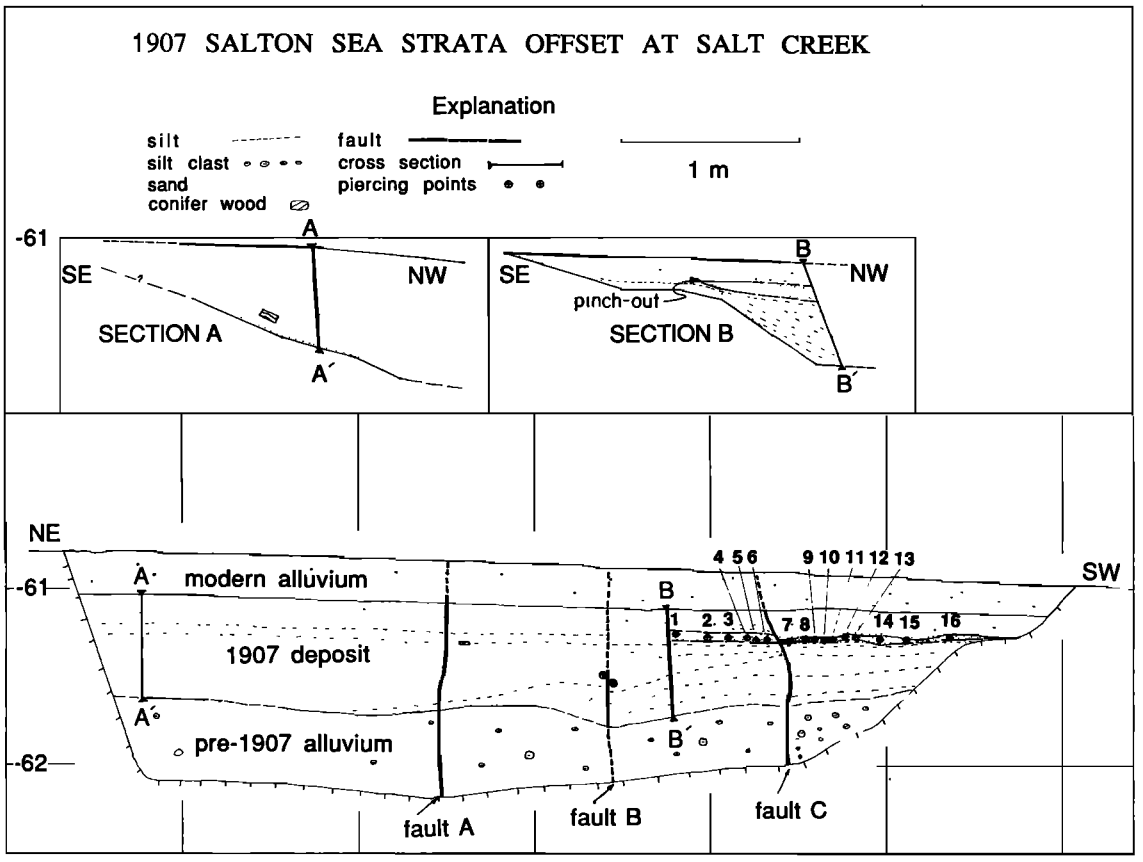

Fig. 11. Surveyed log of trench exposures at Salt Creek. Large cross section is roughly perpendicular to the faults. Numbers 1–16 show where measured cross sections cut roughly parallel to the fault intersect this cross section. Piercing line used to document offset across fault C was the pinchout of the stratum containing the circled crosses.

October 1, 1906, to July 1, 1908 [*U.S. Geological Survey*, 1960].

Figure 11 is a surveyed log of the exposure sketched in Figure 10. Channel fill and underlying alluvium are broken by the fault zone. The exposure is roughly perpendicular to the strike of the three faults that constitute the zone and is nearly parallel to the edge of the channel. The edge of the channel fill is about a meter and a half behind the plane of the exposure. The shape of the channel edge is shown in sections A and B.

The offset of the lacustrine channel fill across the principal fault plane (fault C) was determined by serial excavation of cross sections within the lacustrine unit. In each cross section, a pinchout within the channel fill (indicated on Figure 11, section B) was precisely located above a sandy silt laminae and below a coarser and more poorly sorted topset sand laminae. From these data, we constructed the map in Figure 12. Dextral offset across fault C is 120 ± 20 mm. The uncertainty is not a statistical estimate but rather an estimate that reflects the range of possible offsets, given the irregularities of the pinchout.

A piercing point similar to that measured across fault C was not displaced laterally across fault B but exhibits dip slip of about 40 mm, down on the northwest. The position of the pinch-out was surveyed on either side of the fault, and these points are plotted as dots in Figures 11 and 12.

Dextral slip across fault A was determined to be 30 ± 4 mm from the matching sides of a small pull-apart that formed within the channel fill at a dilatational jog in the fault (Figure 13). No measurable dip slip occurred across this fault or across fault C at the site of the slip measurements.

Calculation of an average slip rate. Together, these three faults have offset the historical lacustrine deposits 150 ± 21 mm dextrally and 40 mm vertically. The time between deposition of the sediment in October 1906 to July 1908 and excavation in April 1987 is 80.4 ± 0.9 years. The average slip rate calculated from these values is 1.9 ± 0.1 mm/yr.

The 300-Year Slip Rate From the Northeastern Flank of the Salton Sea

At Ferrum (Figure 1) we have documented the offset of a geological unit that was deposited about 300 years ago. We chose "Ferrum" as the site name because the locality is only a half kilometer north of the "Ferrum" siding of the Southern Pacific Railroad.

At the Ferrum site the San Andreas fault crosses a stubby promontory that juts southwestward toward the Salton Sea (Figure 14). The surface of the promontory consists predominantly of coarse sand and a one-pebble-thick layer that we interpret to be lag deposit produced by aeolian erosion. The shallow subsurface deposits that are exposed in channels around the nose of the bar and in excavations at the site consist of basinward dipping beds of gravelly sand. The nature and sedimentary structure of the deeper internal deposits of the promontory have not been observed, so their nature can only be inferred from the shape of the promontory and its setting. The promontory is probably constructed

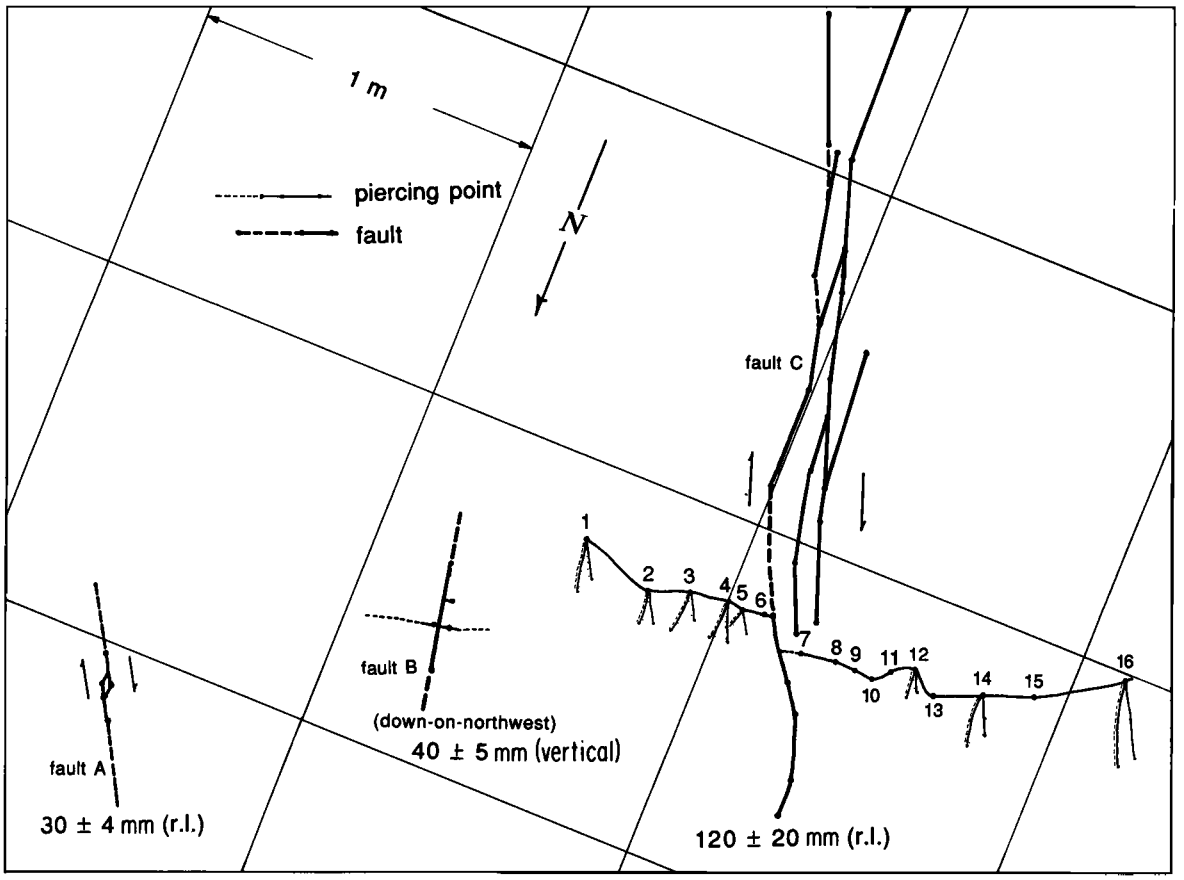

Fig. 12. Map of faults exposed in excavation of post-1907 channel offset at Salt Creek. Shown are a pull-apart with 30 mm offset across fault A, the position of piercing points offset vertically across trace B, and the trace of a reference line offset 120 mm across fault C. The cross sections used to construct the offsets are shown by dots and near fault C are numbered. The cross-sectional shape of the pinchout that is offset across fault C is drawn adjacent to the map position of the respective survey points. Note that the zone of faulting is only about 2 m wide. Amounts of slip shown are for time period 1907–1987.

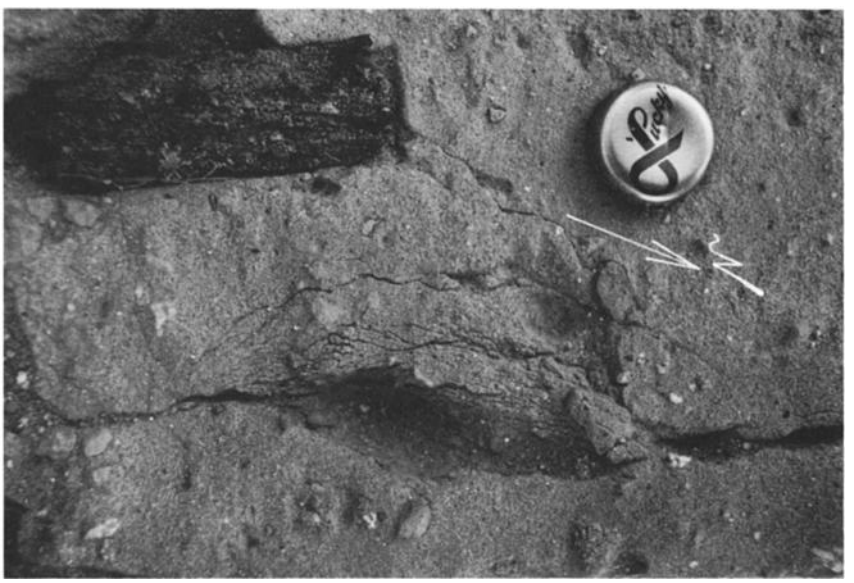

Fig. 13. Photo of pull-apart used to determine the offset across fault A at Salt Creek. Dark rectangular feature at lower left is milled wood imbedded in the lacustrine sediment. Offset is 30 ± 4 mm. Beverage cap is about 25 mm in diameter.

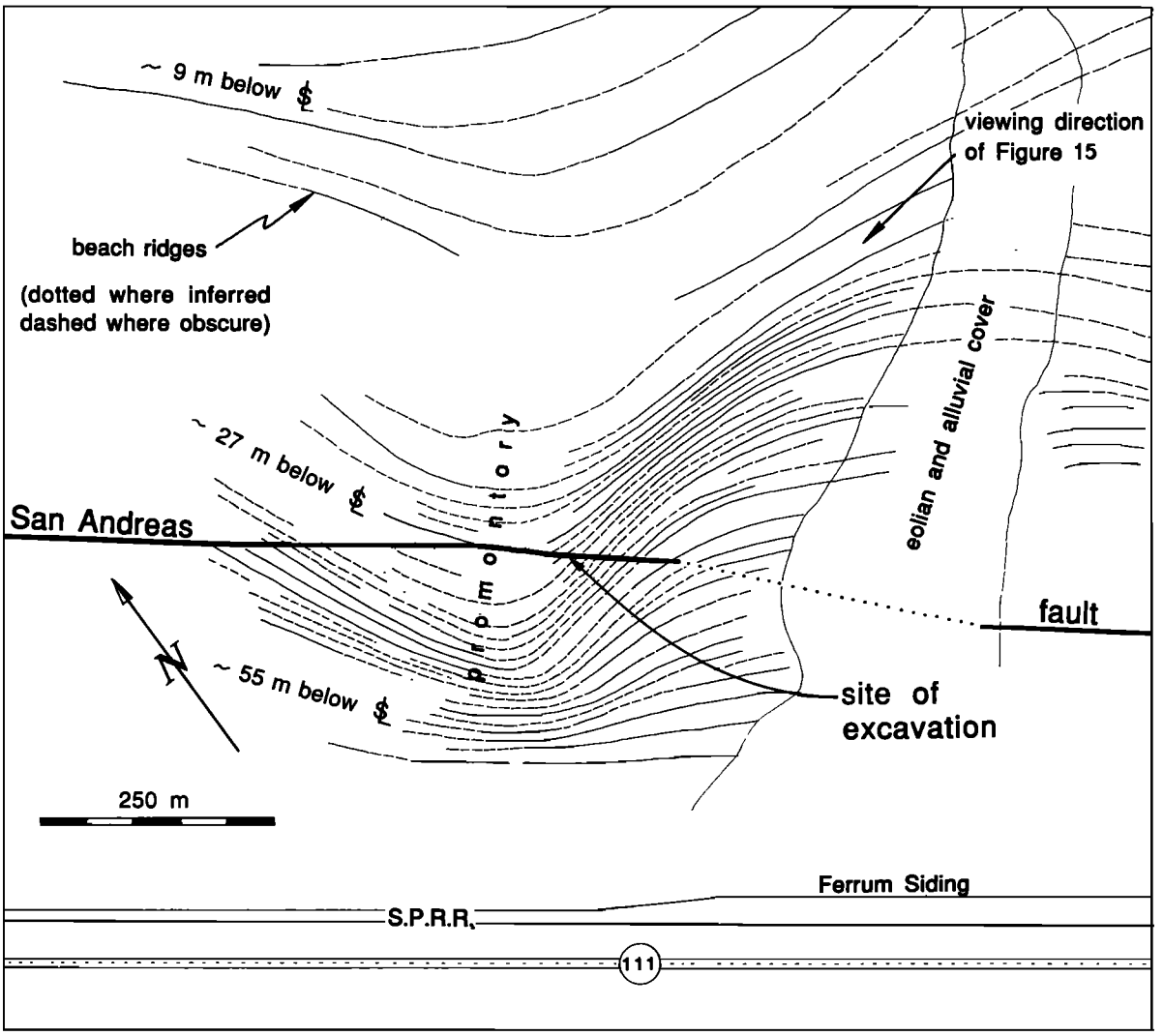

Fig. 14. Map of the Ferrum site. The locations of beach ridges are interpreted from aerial photographs. All elevations are below sea level.

of sand and gravel that was entrained in longshore currents of Lake Cahuilla; it is attached to a larger bar that trends southeastward. The lakeward projection of the promontory may reflect convergence of longshore currents in this area, which would be consistent with the observation that the dominant winds of the Coachella Valley are from the west-northwest, whereas winds out of the west-southwest dominate in the Imperial Valley [*Arnal*, 1961].

Regardless of the origin of the promontory, its surface is ornamented by at least 40 small, nearly continuous, horizontal sand and gravel bands and associated vegetation lines (Figures 14 and 15). These bands are about $\frac{1}{2}$–1 m in height and 2–4 m in width. They have been modified locally by erosion and are most pronounced where groups of plants protect them. Small channels dissect the bands in many places.

The bands consist of beach deposits and represent short still stands of the surface of Lake Cahuilla. The good preservation of these very fragile features strongly suggests that they formed during the most recent desiccation of the lake, about 300 years ago. The average difference in elevation between adjacent ridges is about 1.3 m. Because evaporation occurs most rapidly in the hot summer months, the ridges may well represent about 40 individual wintertime levels of the lake. Some ridges with small vertical separation may have formed during intense summer storms.

The San Andreas fault traverses the promontory at Ferrum and cuts across the beach ridges. On the southeastern flank of the promontory the fault crosses the ridges at oblique angles. A narrow vegetation alignment and discontinuous fault scarps reveal the location of the primary fault trace on the promontory (Figure 15). The position of the principal active fault trace is also known from stone cairns, which mark the locations of minor fault slippage triggered by the Imperial Valley earthquake of 1979 [*Sieh*, 1982].

Stratigraphy of the beach and nearshore deposits at the excavation. Horizontal offset of the beach bands is not geomorphically evident, either from the ground or from aerial photographs; however, the subdued nature of the features and their degree of preservation preclude resolution of any slippage less than about 1.5 m. Because slippage of less than about 1.5 m is not geomorphically detectable, we excavated between two of the recessional beach ridges at the fault in order to identify stratigraphic piercing points and

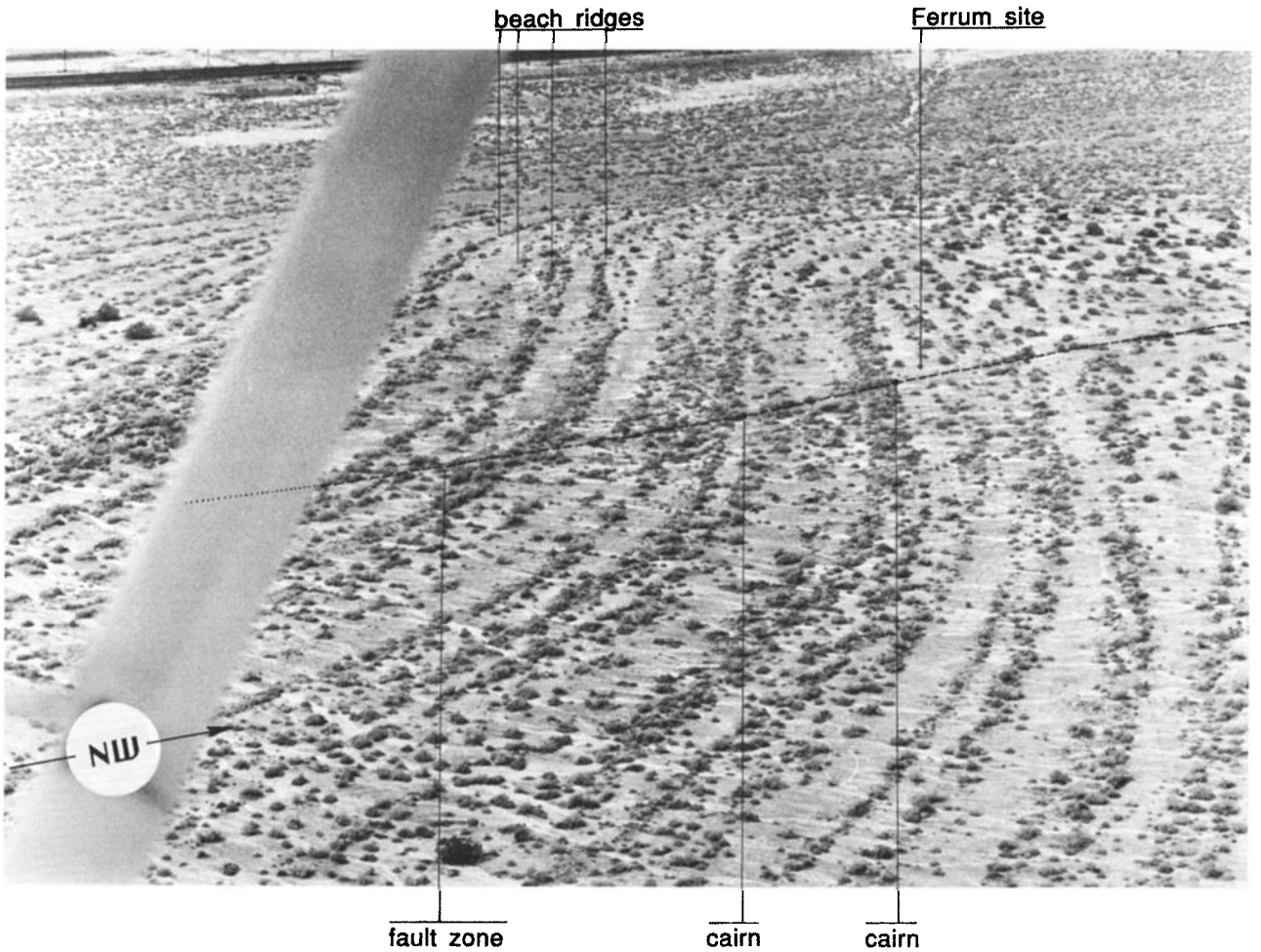

Fig. 15. Oblique aerial photograph of Ferrum site. View is from the east. See Figure 14 for approximate viewing position.

measure their offset. The exact location of our excavation is indicated on both Figures 14 and 15.

Figure 16 is the log of a trench cut parallel to and about 1 m northeast of the fault between two of the beach ridges. Three units are visible. The uppermost unit (unit 1) is poorly sorted silty pebbly sand and is commonly about 10 cm thick. The poor sorting of the unit and its position immediately beneath the ground surface indicate a predominantly colluvial origin.

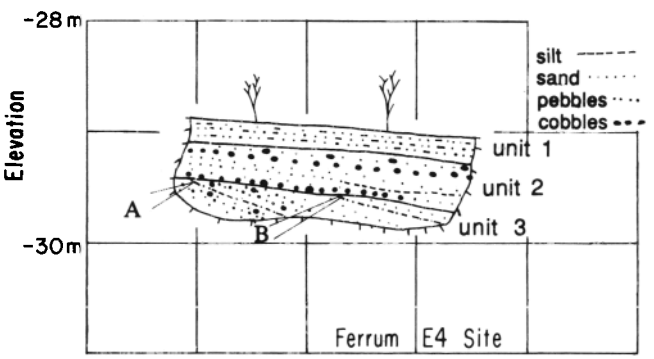

Fig. 16. Cross-sectional view of exposure E4, cut parallel to the San Andreas fault (no vertical exaggeration). A and B are the two reference lines exposed in the plane of the excavation. These are offset across the fault.

The intermediate unit in Figure 16 (unit 2) is a pebble-cobbly sand which contains moderately persistent, flat-bedded silty sand laminations. Sorting of sand within unit 2 is locally good, but moderately poor sorting characterizes the unit as a whole. Unit 2 dips about 5°, parallel to the ground surface and truncates underlying beds of unit 3. Pockets of pebble gravel are present at the base of unit 2. The gravels are most likely derived from the underlying unit through removal of fines.

The lowest unit exposed in the Ferrum excavations is unit 3. Unit 3 consists of well-laminated, well-sorted medium to coarse sand and abundant laminae of granule and pebble sand. Laminae within the unit dip 20°–33° lakeward. Laminae of silty very fine sand define the boundaries of coarser beds.

The geometry of units 2 and 3 suggests that unit 2 is a deposit of the inner beach zone and that unit 3 originated in an adjacent nearshore zone. The planar but gently dipping character of unit 2 is consistent with deposition on a beach face (that is, a swash zone) [*Thompson*, 1937; *Clifton et al.*, 1971; *Komar*, 1976]. Unit 3 resembles the seaward dipping foreset-bedded "inner planar" portion of the nearshore

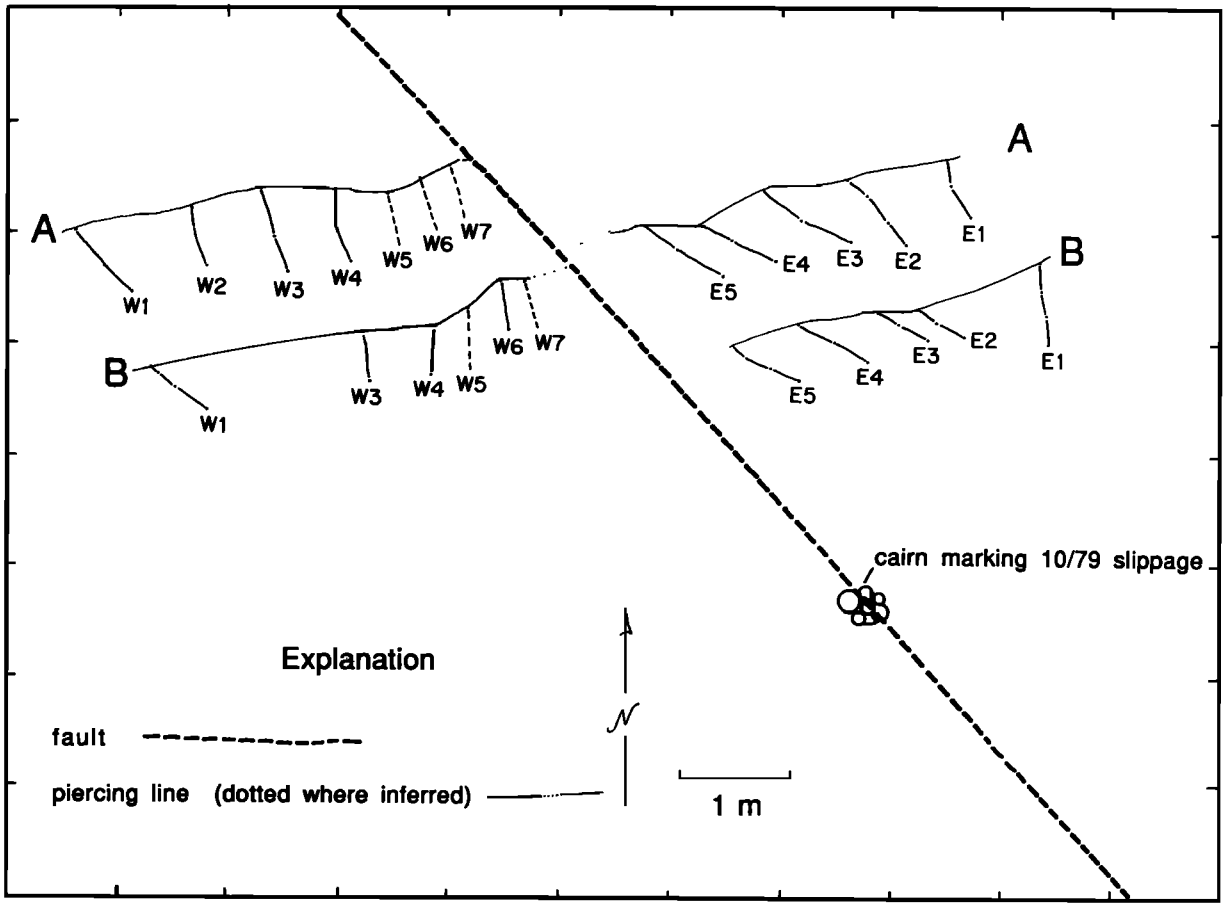

Fig. 17. Map of offset reference lines at Ferrum. Reference lines are offset 1.1 ± 0.15 m. Dash-dot lines represent the trace of the bed that forms the piercing line in each mapped exposure.

zone, seaward of the swash zone, as described by *Clifton et al.* [1971].

As the surface of the lake fell by evaporation, the nearshore deposits of unit 3 found themselves above wave base. Erosion of the upper parts of these sands by wave action ensued. Beach zone deposits of unit 2 were then deposited upon the eroded surface of unit 3. This is the relationship one would expect to see in the nearshore and beach deposits of a highly energetic desiccating lake (Appendix 3). In the intertidal analogue, planar, seaward dipping nearshore sands formed during high tide are truncated by swash zone deposits as tide falls [*Clifton et al.*, 1971, Figure 18]. Thus we believe that units 2 and 3 were deposited during the latest dessication of Lake Cahuilla. The colluvial deposits of unit 1 were deposited in the years, decades, and centuries following the passage of lake level below the top of the beach zone deposits.

The veracity of our interpretation of units 2 and 3 is critical to the use of the upward truncations of laminations in unit 3 to determine offset across the fault. We use the lines traced by two silty-sand laminae of unit 3 upon the upper, eroded surface of unit 3 as reference lines to measure offset across the fault. If units 2 and 3 are very nearly the same age, then it is reasonable to assume that no fault slip occurred between the times of their deposition. If, however, unit 3 represents deposits of an older lake, then substantial slip may well have occurred between deposition of units 2 and 3, and the separation of the reference lines probably would not represent actual offset.

Excavation of the offset reference feature. We made a series of fault-parallel excavations to expose and measure the offset of the reference lines formed by the trace of laminations across the upper surface of unit 3. The area of excavation extended 10 m normal to the fault and 5 m parallel to it. Twelve fault-parallel exposures were described. The exposures were cut at the angle of repose of the loose sand beds.

The features used are labeled A and B in Figure 16. The plan view geometry of these two reference features appears in Figure 17. Details of grain size and stratigraphic geometry are unique, and so no reasonable doubt exists that the correlation of reference lines across the fault is valid. Reference line A is the top of a sandy silt lamina sandwiched between lakeward dipping beds of coarse to granule and small pebbly sand, whereas reference line B is sandwiched between beds of medium to granule sand. Further confirmation of the validity of the correlations is the occurrence of a persistent silt lamina within unit 2 (Figure 16) in a similar relationship to features A and B on both sides of the fault.

Figure 17 documents that reference features A and B are offset 1.15 ± 0.15 and 1.15 ± 0.25 m, respectively. The uncertainties are estimated by projecting reference lines to the fault using the maximum angular deviation of the two reference lines. Propagation of the uncertainties of measure-

ments A and B yields a measurement uncertainty of ±0.15 m.

We found no evidence of secondary faulting; thus the total fault slippage appears to be 115 cm. That no additional fault traces have carried significant slippage during the past 300 years is consistent with the observation of *Sieh* [1982] that aseismic slippage in 1979 was limited to a linear zone that intersects the excavation site as shown in Figure 17. A fault bend or step is present about 300 m south of the site (Figure 14), and it may therefore be argued that a fault splay extends from the southeast, parallel to the branch we investigated. We believe, however, that if an active branch is present to the southwest of the Ferrum excavation, it probably does not slip aseismically.

Age of the offset reference lines. Units 2 and 3 most probably were deposited during the latest period of desiccation of Lake Cahuilla, as the level of the lake fell through the elevation of the site. A youngest plausible date for the units, A.D. 1738, is calculable from de Anza's observation that no lake existed at the time of his visits in 1774 and 1775 [*Bancroft*, 1884; *Bolton*, 1930]. Given that the Ferrum site is 56 m above the deepest part of the basin and assuming that annual rates of drawdown during the latest desiccation of Lake Cahuilla are similar to the 1.55 m/yr rate of drawdown of the Salton Sea between 1907 and 1913 (Appendix 2), about 36 years elapsed between the time the lake level stood at the Ferrum site and time of complete desiccation. Hence the youngest plausible date for units 2 and 3 is A.D. 1738.

An oldest plausible date of deposition of units 2 and 3 can be derived from radiocarbon dates obtained for material drowned at the Indio site by the filling of the latest lake, presented above. Those data indicate that the lake must have begun desiccation no earlier than A.D. 1663 ± 22. The high stand elevation of the latest filling was 41 m above the Ferrum site. Assuming the same rate of drawdown as before, we calculate that 27 years must have elapsed between the beginning of lake drawdown and passage of the lake surface through the Ferrum site. The maximum date of these offset deposits is therefore, A.D. 1690 ± 22 and the range of plausible dates is 1703 ± 35.

Calculation of an average slip rate. The reference features at Ferrum are 284 ± 35 years old, and they display an offset of 1.15 ± 0.15 m. Thus the average slip rate between the time of their deposition and excavation is 4.0 ± 1.0 mm/yr [*Taylor*, 1982, p. 49].

DISCUSSION

Figure 18 consists of two graphs. One graph displays slip data from near Indio and the other displays slip data from near the Salton Sea. These data suggest that these two portions of the southernmost San Andreas fault have been slipping at low rates throughout the past three centuries.

Near Indio the modern rates of about 2 mm/yr, measured at the Indio Hills and Dillon Road alignment arrays, are indistinguishable from the average rate measured at the 40-year-old wasteway. The average rate during the past three centuries is about 4 mm/yr. Near the Salton Sea the modern rate of 4 mm/yr, measured by the Mecca Beach creepmeter, is similar to an average rate of about 2 mm/yr, which spans the twentieth century, and to a 4 mm/yr rate, which spans the past three centuries.

Differences in these rates are small, and it is difficult to evaluate their causes or significance. One could hypothesize that the slip rate at both of the sites represented in Figure 18 has remained constant through the past 300 years and that the differences result from the geographic separations of the sites. The 0–4 mm/yr range of rates recorded by modern creep meters and alignment arrays along this fault segment certainly supports the hypothesis that the differences from site to site do not indicate temporal variation in slip rate.

The fact that apertures and site conditions differ widely among the data presented in Figure 18 also allows this interpretation. For example, compare the nature of the data collected from Salt Creek, Mecca Beach and Ferrum. The 300-year-averaged rate from Ferrum represents solely the amount of slip that has occurred across the one, narrow fault plane at the site and does not include any distributed warp in

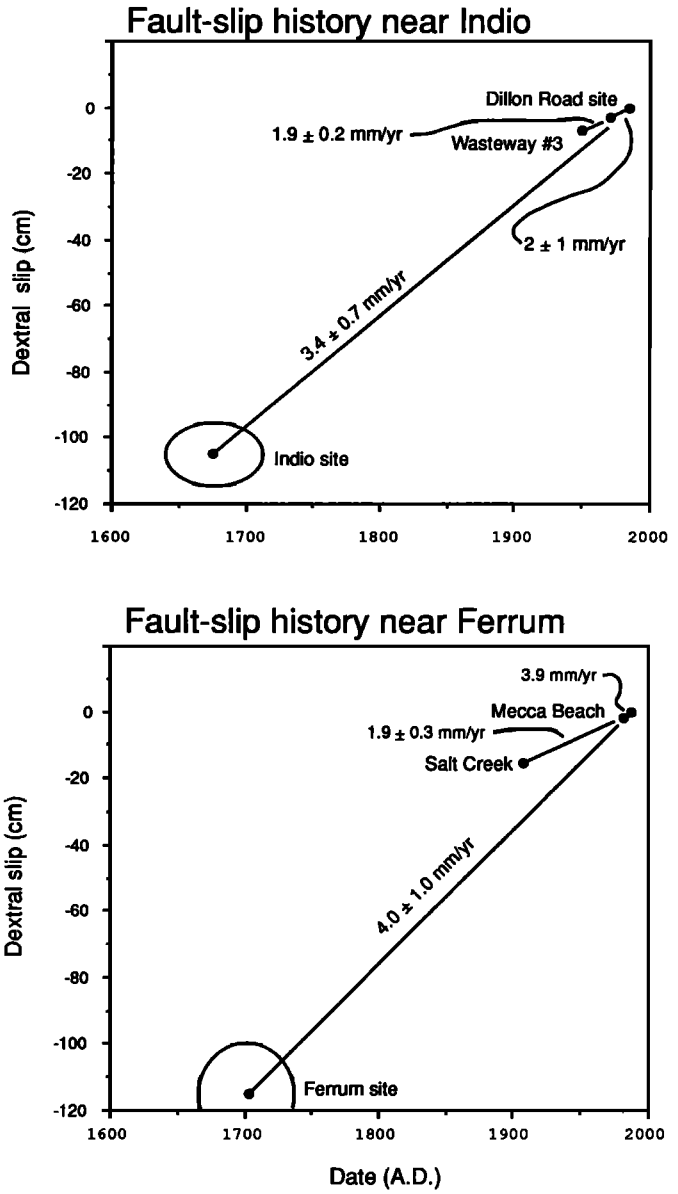

Fig. 18. Three-hundred-year history of slippage across the San Andreas fault (top) in the vicinity of the Indio site and (bottom) on the northeastern flank of the Salton Sea. Uncertainties in slip reflect the estimated measurement uncertainty and, in the case of the oldest offsets, the 95% likelihood uncertainty.

the blocks adjacent to the fault. Likewise, the 80-year-averaged rate from Salt Creek is based upon a measurement of the brittle offset across three fault traces in a 2-m-wide zone. The 7-year-average rate from Mecca Beach includes shear localized on the fault plane and distributed as warp up to 3 m away from the fault trace. One cannot rule out the possibility that rates measured at these sites would be identical if measurements had been made across much wider apertures. Because of these uncertainties, we do not attempt to assess the significance of the small differences in the rates presented in Figure 18.

However, the similar slip rates determined for periods that range from a decade to three centuries is worthy of discussion. Ostensibly, these data indicate that fault creep has been occurring along the southernmost reach of the San Andreas fault at rates of up to 4 mm/yr throughout the past three centuries. Alternative interpretations are possible, however. Rates may have varied markedly but over periods too short to be resolved by these data. For example, the 3.4 mm/yr average rate determined from the Indio site for the past 300 years may consist of a 50-cm seismic slip event superimposed upon a steady state creep rate of about 2 mm/yr.

If appreciable seismic slip does constitute part of the slip history of Indio or Ferrum during the past 300 years, it must have occurred prior to about 1877, when the Southern Pacific Railroad was completed in the valley [*Agnew*, 1985]. It would also have to be associated with moderate or small earthquakes, not a large one. This judgment is derived from the fact that the small amount of slip measured at Indio and at Ferrum is inconsistent with coseismic slip during an earthquake greater than about magnitude 7 [*Slemmons*, 1977].

For this reason, the large earthquake of December 8, 1812, which *Jacoby et al.* [1988] have recently placed along the San Andreas fault near Los Angeles, is unlikely to have been associated with seismic slippage along this segment. With the exception of one dubious account of faulting at Dos Palmas (7 km east of Mecca Beach, Figure 1) in 1868 [*Townley and Allen*, 1939], no reports of moderate earthquakes exist for the period of historical record. This may well mean that no moderate earthquakes have been produced by this segment since at least 1790. Such an interpretation is risky, however, because the historical record of the late eighteenth and early to middle nineteenth centuries is incomplete [*Agnew*, 1985, also personal communication, 1987].

The latest large earthquake to have been produced by this segment of the San Andreas fault appears to have occurred in A.D. 1676 ± 35, during the latest highstand of Lake Cahuilla [*Sieh*, 1986, also unpublished data, 1990]. At the Indio site, fault 2 (Figure 4) clearly displays dip slip of up to 10 cm during deposition of the topset beds of the latest lake bar (K. E. Sieh, unpublished data, 1990). Fault 1 clearly shows dextral offsets of about 2 m at this same time. Such a large dextral offset is typically associated with earthquake magnitudes greater than 7 and rupture lengths of at least several tens of kilometers [*Slemmons*, 1977]. Afterslip during the years following this earthquake could well be part of the 1-m channel offsets recorded at the Indio site.

The reason for long-term, low-level creep along this segment of the San Andreas fault is unclear. *Bilham and Williams* [1985] have noted that creep has been documented only where the trace of the fault strikes more westerly than its regional trend. They point out the thick accumulation of modern alluvial gravel across the intervening segments and suggest that this may cause distribution of creep across a wide zone. These observations fail to account for the fact that similar behavior is not observed along the other seismogenic segments of the San Andreas fault in southern and northern California.

One plausible mechanism for shallow aseismic stress relief is suggested by the experimental work of *Marone and Scholz* [1988]. They show that loose gougelike materials exhibit velocity-strengthening behavior. That is, their resistance to shear increases with shear velocity. Velocity-strengthening behavior inhibits the instability required for seismogenic failure and is proposed as the fundamental cause of all types of aseismic fault slippage. Unstable stick-slip behavior is observed in gougelike materials as they become sufficiently consolidated; thus the experimental data of Marone and Scholz indicate that in common lithologies, fault creep is restricted to shallow depths. The lack of observed stable sliding along other faults and many other segments of the San Andreas fault is not explained by this hypothesis, nor is the observation of creep throughout the upper 10 km of the fault in central California.

We offer the hypothesis that slow, quasi-continuous aseismic slip occurs along this segment of the fault because of high pore pressures in the coarse sediments that abut the fault. Such a condition is plausible, given the abundance and great thickness of coarse clastic sediments southwest of the fault [*Allen*, 1957; *Sylvester and Smith*, 1976], the intercalation of these with relatively impermeable silts and clays, and the opportunity for the development of overpressures due to compaction and tectonic deformation of the sediments. High pore pressures would reduce the effective normal stress on the fault and thus reduce its strength. At greater depths, where consolidated and relatively impermeable crystalline rocks abut the fault, the strength of the fault would be higher, and the fault plane would be locked between large earthquakes. We propose that the presence of the locked patch prevents the weak upper few kilometers of the fault from slipping at rates closer to the long-term rate of slip of about 25 mm/yr. This mechanism could apply not only to the San Andreas fault in the Coachella Valley but also to the Imperial, Coyote Creek, and Superstition Hills faults in the Imperial Valley (Figure 1) where similar geologic conditions exist.

The plausibility of such a hypothesis can be assessed by comparing a theoretical model to actual conditions. First, we calculate the surficial strain rate across the fault, given a reasonable slip rate below a locked patch, the base of which is at depth D. Then, we use that strain rate and the observed creep rates to determine the depth of the top of the locked patch. Finally, we compare the calculated depth with the depth to basement in the Coachella Valley. *Savage and Burford* [1973, p. 832] suggested the modeling of interseismic surficial strain rate profiles across strike-slip faults by means of a buried screw dislocation in an elastic half-space. In their analysis they assumed no slippage of the fault above a certain depth D. *Savage and Burford* [1973, p. 832] also recognized that imposing motion on the fault was a convenient simplification of the more complicated driving mechanism in which "the plates slip past one another in response to shear stresses that presumably originate from the drag of

TABLE A1. Data Ranges for Filling of Latest Lake

Sample						
Field (CAH-)	Lab (UW-)	^{14}C Age ($\pm 1\sigma$)	$\delta^{13}C$ (‰)	Isotopically Corrected Age		Dendrochronologically Calibrated Age (A.D.) (95% Confidence Limits)
80-3	642	260 ± 45	−26.79	231 ± 45	214 ± 33	1641–1684
						1725–1807
80-4	643	210 ± 50	−26.11	192 ± 50		1933–1955

mantle convention currents upon the bottom of the lithospheric plates." Following *Weertman and Weertman* [1964], they proposed that the surface strain rate

$$\dot{\tau} = \mu V_{pl}/\pi D \quad (1)$$

where μ is the shear modulus, D is the depth above which no slip occurs, and V_{pl} is the rate of slip on the fault below the depth of locking.

Knopoff [1958] showed that the surficial slip rate of a fault that was free to slip above a locked portion could be calculated as

$$\dot{\delta}_{surf} = 2\frac{\dot{\tau}}{\mu} d \quad (2)$$

where $\dot{\delta}_{surf}$ is the surficial slip rate, $\dot{\tau}$ is the strain rate calculated from (1), and d is the depth of the freely slipping crack. Equations (1) and (2) combine to yield

$$\dot{\delta}_{surf} = \frac{2}{\pi} V_{pl} \frac{d}{D} \quad (3)$$

In our particular case, we know $\dot{\delta}_{surf} \approx 2$–4 mm/yr, and we believe that $V_{pl} \approx 23$–35 mm/yr [*Keller et al.*, 1982; *Sieh*, 1986]. Estimates of D vary between about 5 and 15 km. Two-dimensional models of geodetic data by *King and Savage* [1983] fit the data best if a value of about 5 km is used. Alternatively, if one assumes that D is equivalent to the maximum depth of earthquake hypocenters, a value of about 10 km must be used for all of the Coachella segment, except near its northwestern end where events occur at depths as great as 15 km (L. Jones, personal communication, 1989).

If we choose central values of 3 mm/yr, 30 mm/yr, and 10 km for $\dot{\delta}_{surf}$, V_{pl} and D, the depth to the base of the slowly creeping part of the fault, d, is calculated to be 1.6 km. The uncertainties in V_{pl} and D and in the range in observed values of $\dot{\delta}_{surf}$ allow this depth to be as as shallow as 0.6 km or as deep as 2.7 km.

This theoretical result supports our hypothesis that creep is limited to the portions of the fault that cuts the sediments of the valley, because the thickness of sediment in the block southwest of the fault is estimated to be within this range. Based upon a seismic refraction experiment, *Kohler and Fuis* [1986, Figure 11] estimate a depth to basement of about 2 km along the segment of the fault east of the Salton Sea. *Biehler et al.* [1964, Figure 6] estimate a depth to basement of about 1.3 km in the Coachella Valley based upon a seismic refraction profile shot parallel to and 4 km southwest of the Banning fault. They caution, however, that a nearby well penetrated 2 km of sediment without reaching crystalline basement. Their gravity data suggest that sediments could be between 3 and 8 km thick farther southeast, near Mecca. (This wide range in values is due to the large uncertainty in the appropriate density contrast to use in modeling the gravity data.) *Sylvester and Smith* [1976] seem to favor a total sediment thickness of about 1.8 km southwest of and adjacent to the fault, based upon their knowledge of stratigraphic thicknesses within the fault zone.

From these sparse data, a reasonable estimate of the thickness of sediments along the fault would be in the range of 1.3–3 km. This certainly overlaps the 0.6–2.7 km range calculated as the depth to the base of the aseismically creeping part of the fault. Thus we conclude that a weak upper 1 or 2 km fault zone could be produced by high pore pressures in the sediments that abut the fault.

CONCLUSIONS

Our comparison of creep rates averaged over the past one decade to three centuries suggests that creep at rates of 2–4 mm/yr is a long term characteristic of the Coachella Valley segment of the San Andreas fault. This implies that low-level creep is not a short-term precursor to major seismic failure there. We hypothesize that the creep is restricted to the shallow portion of the fault and that this phenomenon is produced by high pore pressures in the sediments adjacent to the fault.

APPENDIX 1

The data ranges for filling of the latest lake have been calculated from the ^{14}C data on peat given in Table A1.

The two samples were analyzed in the radiocarbon laboratory of A. W. Fairhall, Department of Chemistry, University of Washington, Seattle. The $\delta^{13}C$ values were determined in the laboratory of M. Stuiver, Quaternary Isotope Laboratory, University of Washington. Dendrochronologic calibration of the ages was done with the calibration program of *Stuiver and Pearson* [1986].

APPENDIX 2

The Salton Sea evaporation rate between April 1, 1907, and April 1, 1913, was calculated by *Cory* [1913] and *Robson* [1913]. They used data from *U.S. Geological Survey* [1913] and H. T. Cory's personal records to estimate that the input of agricultural water into the sea during 1907–1913 was 1.31 m. This was added to the 7.86-m lake level fall during this period yielding a corrected basin drawdown of 9.27 m and an annual evaporation rate of 1.55 m/yr. At this rate, just 63 years are required for complete evaporation of the lake. Recessional shorelines at Ferrum have an average spacing of 1.32 m. When we discount clearly intermediate-spaced

shorelines that were probably formed during severe summer storms and may thus represent less than a full year's recession, the average vertical spacing is 1.52 m. This is in close agreement with the 1907–1913 data. We cannot, of course, exclude the possibility that irrigation input into the basin during 1907–1913 was underestimated.

APPENDIX 3

That Lake Cahuilla was a highly energetic lake is demonstrated by the modern occurrence of wind velocities that regularly exceed 50 km/h over the lake bed. While the lake stood at Ferrum, winds from the southeast and northwest acted across a fetch of 30–40 km. During wind storms deep water waves are calculated to have reacted a meter in amplitude [*King*, 1972], and beach energetics regularly approached those of moderately high-energy marine beaches. Large wave energies are also evidenced by the scale of beach cliff, bar, and berm development along the lake's eastern perimeter [*Norris et al.*, 1979]. Given that beach conditions were roughly analogous to those of marine beaches, it is justified to compare the Lake Cahuilla beach sediments to marine analogues such as those described by *Clifton et al.* [1971].

Acknowledgments. We particularly appreciate the cooperation of the owners and wardens of lands on which we made excavations and surveys. P. Ames permitted us to work at the Indio site, W. Gardner provided access to Wasteway 3, and supervisors of Salton Sea State Park allowed our work at the Ferrum and Salt Creek sites. We are also grateful to N. Brown, K. W. Hudnut, M. F. Hudson, P. H. Molnar, A. Thomas, and S. G. Wesnousky for their able field assistance. R. Dmowska and J. Rice shepherded us in our calculations. Discussions with C. R. Allen, R. G. Bilham, K. F. Evans, C. H. Scholz, W. D. Stuart, and L. R. Sykes were also helpful. An early version of the manuscript was significantly improved by the reviews of N. Christie-Blick and L. R. Sykes. C. R. Allen provided Mecca Beach creep meter data before publication. Caltech creep meters and alignment arrays are currently supported by U.S. Geological Survey Earthquake Hazards Reduction Program grant 14-08-0001-G1177 to C. R. Allen and K. E. Sieh. Part of Williams' support during the period of this study came from U.S. Geological Survey Earthquake Hazards Reduction Program grant 14-08-0001-G-948 to L. R. Sykes. A total station used to document most of the sites presented here was purchased with funds from the W. M. Keck Foundation and the U.S. Geological Survey Earthquake Hazards Reduction Program grant 14-08-0001-G1177. This study was funded principally by U.S. Geological Survey Earthquake Hazards Reduction Program grant 14-08-0001-G1098. Field data in the vicinity of the Indio site were collected primarily by K.E.S., and field data from the area on the eastern flank of the Salton Sea were collected primarily by P.L.W. This is contribution 4763 of the Division of Geological and Planetary Sciences, California Institute of Technology, Pasadena, California.

REFERENCES

Agnew, D. C., Evidence on large southern California earthquakes from historic records, *U.S. Geol. Surv. Open File Rep., 85-507*, 76–90, 1985.

Allen, C. R., San Andreas fault zone in San Gorgonio Pass, southern California, *Geol. Soc. Am. Bull., 68*, 315–350, 1957.

Allen, C. R., The tectonic environments of seismically active and inactive areas along the San Andreas fault system, Proceedings of Conference on Geological Problems of the San Andreas Fault System, edited by W. R. Dickinson and A. Grantz, *Stanford Univ. Publ. Geol. Sci., 11*, 70–82, 1968.

Allen, C. R., M. Wyss, J. N. Brune, A. Grantz, and R. Wallace, Displacement on the Imperial, Superstition Hills, and San Andreas faults triggered by the Borrego Mountain earthquake, The Borrego Mountain Earthquake, *U.S. Geol. Surv. Prof. Pap., 787*, 87–104, 1972.

Arnal, R. E., Limnology, sedimentation, and microorganisms of the Salton Sea, California, *Geol. Soc. Am. Bull., 72*, 427–478, 1961.

Bancroft, H. H., History of California, vol. 1, 1542–1800, in *The Works of Herbert Howe Bancroft*, vol. XVIII, A. L. Bancroft, San Francisco, Calif., 1884.

Bilham, R., and P. Williams, Sawtooth segmentation and deformation processes on the southern San Andreas fault, California, *Geophys. Res. Lett., 12*, 557–560, 1985.

Bolton, H. E., *Anza's California Expeditions*, vol. 1, 529 pp., University of California Press, Berkeley, 1930.

Clark, M. M., Map showing recently active breaks in the San Andreas fault and associated faults between the Salton Sea and Whitewater River–Mission Creek, California, *U.S. Geol. Surv. Misc. Invest. Map, I-1483*, 2 sheets, 1984.

Clifton, H. E., R. E. Hunter, and R. L. Philips, Depositional structure and process in the nonbarred, high energy nearshore, *J. Sediment. Petrol., 41*, 651–670, 1971.

Cory, H. T., Irrigation and river control in the Colorado River Delta, *Trans. Am. Soc. Civ. Eng., 76*, 1204–1450, 1913.

Jacoby, G. C., P. R. Sheppard, and K. E. Sieh, Irregular recurrence of large earthquakes along the San Andreas fault: Evidence from trees, *Science, 241*, 196–199, 1988.

Jennings, C. W., Fault map of California, 1 sheet, Calif. Div. of Mines and Geol., Sacramento, 1975.

Keller, E. A., M. S. Bonkowski, R. J. Korsch, and R. J. Shiemon, Tectonic geomorphology of the San Andreas fault zone in the southern Indio Hills, Coachella Valley, California, *Geol. Soc. Am. Bull., 93*, 46–56, 1982.

Keller, R. P., C. R. Allen, R. Gilman, N. R. Goulty, and J. A. Hileman, Monitoring slip along major faults in southern California, *Bull. Seismol. Soc. Am., 68*, 1187–1190, 1978.

King, C. A. M., *Beaches and Coasts*, 570 pp., Edward Arnold, London, 1972.

King, N. E., and J. C. Savage, Strain rate profile across the Elsinore, San Jacinto, and San Andreas faults near Palm Springs, California, 1973–1981, *Geophys. Res. Lett., 10*, 55–57, 1983.

Knopoff, L., Energy release in earthquakes, *Geophys. J. R. Astron. Soc., 1*, 44–52, 1958.

Kohler, W., and G. Fuis, Travel-time, time-term, and basement depth maps for the Imperial Valley region, California, from explosions, *Bull. Seismol. Soc. Am., 76*, 1289–1303, 1986.

Komar, P. D., *Beach Processes and Sedimentation*, 429 pp., Prentice-Hall, Englewood Cliffs, N. J., 1976.

Lindh, A. G., Preliminary assessment of long-term probabilities for large earthquakes along selected segments of the San Andreas fault system in California, *U.S. Geol. Surv. Open File Rep., 83-63*, 15 pp., 1983.

Louie, J. N., C. R. Allen, D. C. Johnson, P. C. Haase, and S. N. Cohn, Fault slip in southern California, *Bull. Seismol. Soc. Am., 75*, 811–833, 1985.

Marone, C., and C. H. Scholz, The depth of seismic faulting and the upper transition from stable to unstable slip regimes, *Geophys. Res. Lett., 15*, 621–624, 1988.

Norris, R. M., E. A. Keller, and G. L. Meyer, Geomorphology of the Salton Basin, in *Geological Excursions in the Southern California Area, Annual Field Trip Guide*, pp. 17–46, Geological Society of America, Boulder, Colo., 1979.

Prescott, W. H., M. Lisowski, and J. C. Savage, Velocity field along the San Andreas fault in southern California, *Eos Trans. AGU, 68*, 1506, 1987.

Raleigh, C. B., K. E. Sieh, L. R. Sykes, and D. L. Anderson, Forecasting southern California earthquakes, *Science, 217*, 1097–1104, 1982.

Robson, F. T., Discussion: Irrigation and river control in the Colorado River Delta, *Trans. Am. Soc. Civ. Eng., 76*, 1516–1524, 1913.

Savage, J. C., and R. O. Burford, Geodetic determination of relative plate motion in central California, *J. Geophys. Res., 78*, 832–845, 1973.

Savage, J. C., W. H. Prescott, M. Lisowski, and N. E. King, Strain accumulation in southern California, 1973–1980, *J. Geophys. Res., 86*, 6991–7001, 1981.

Savage, J. C., W. H. Prescott, and G. Gu, Strain accumulation in

southern California, 1973–1984, *J. Geophys. Res.*, *91*, 7455–7473, 1986.

Sieh, K. E., Slip along the San Andreas associated with the earthquake, The Imperial Valley Earthquake of October 15, 1979, *U.S. Geol. Surv. Prof. Pap.*, *1254*, 155–160, 1982.

Sieh, K. E., Slip rate across the San Andreas fault and prehistoric earthquakes at Indio, California (abstract), *Eos Trans. AGU*, *67*, 1200, 1986.

Slemmons, D. B., Faults and earthquake magnitude, *Misc. Pap. S-73-1*, U.S. Army Eng. Waterways Exp. Stn., Vicksburg, Miss., 1977.

Stuart, W. D., Forecast model for large and great earthquakes in southern California, *J. Geophys. Res.*, *91*, 13,771–13,786, 1986.

Stuiver, M., and G. W. Pearson, High precision calibration of the radiocarbon time scale, AD 1950–500 BC, *Radiocarbon*, *28*, 805–838, 1986.

Sykes, L. R., and S. P. Nishenko, Probabilities of occurrence of large plate rupturing earthquakes for the San Andreas, San Jacinto, and Imperial faults, California, 1983–2003, *J. Geophys. Res.*, *89*, 5905–5927, 1984.

Sylvester, A. G., and R. R. Smith, Tectonic transpression and basement-controlled deformation in San Andreas fault zone, Salton Trough, California, *Am. Assoc. Pet. Geol. Bull.*, *60*, 2081–2102, 1976.

Taylor, J. R., *An Introduction to Error Analysis*, 270 pp., Oxford University Press, New York, 1982.

Thompson, W. O., Original structures of beaches, bars and dunes, *Geol. Soc. Am. Bull.*, *48*, 723–752, 1937.

Townley, S. D., and M. W. Allen, Descriptive catalog of earthquakes of the Pacific coast of the United States: 1769 to 1928, *Bull. Seismol. Soc. Am.*, *29*, 1–297, 1939.

Tse, S. T., R. Dmowska, and J. R. Rice, Stressing of locked patches along a creeping fault, *Bull. Seismol. Soc. Am.*, *75*, 709–736, 1985.

U.S. Geological Survey, *U.S. Geol. Surv. Water Supply Pap.*, *300*, 1913.

U.S. Geological Survey, Water supply of the Salton Sea Basin, *U.S. Geol. Surv. Water Supply Pap.*, *1314*, 270 pp., 1960.

Weertman, J., and J. R. Weertman, *Elementary Dislocation Theory*,, Macmillan, New York, 1964.

Weldon, R. J., and K. E. Sieh, Holocene rate of slip and tentative recurrence interval for large earthquakes on the San Andreas fault, Cajon Pass, southern California, *Geol. Soc. Am. Bull.*, *96*, 793–812, 1985.

Williams, P. L., Aspects of the earthquake geology and seismotectonics of the southern San Andreas and related faults, southern California, Ph.D. thesis, 276 pp., Columbia Univ., New York, 1989.

Williams, P. L., and H. W. Magistrale, Slip along the Superstition Hills fault associated with the 24 November 1987 Superstition Hills, California, Earthquake, *Bull. Seismol. Soc. Am.*, *79*, 390–410, 1989.

K. E. Sieh, Division of Geological and Planetary Sciences, California Institute of Technology, Pasadena, CA 91125.

P. L. Williams, Lawrence Berkeley National Laboratory, Berkeley, CA 94720.

(Received September 3, 1988;
revised November 13, 1989;
accepted November 16, 1989.)